Protease-Activated Receptor-1 Inhibition by FR171113 Attenuates Cardiac Remodeling Due to Intermittent Hypoxia

Hideki Imano[1]; Ryuji Kato[1]; Yoshio Ijiri[1]; Takehiro Yamaguchi[2]; Yasukatsu Izumi[3]; Atsuo Nomura[1,4]; Minoru Yoshiyama[2]; Tetsuya Hayashi[1]*

[1]Department of Cardiovascular Pharmacotherapy and Toxicology, Osaka University of Pharmaceutical Sciences, Japan.

[2]Department of Cardiovascular Medicine, Osaka City University Graduate School of Medicine, Japan.

[3]Department of Pharmacology, Osaka City University Graduate School of Medicine, Japan.

[4]Department of Pharmacology, Faculty of Medicine, Osaka Medical College, Japan.

*Corresponding Author(s): Tetsuya Hayashi

Department of Cardiovascular Pharmacotherapy and Toxicology, Osaka University of Pharmaceutical Sciences, Nasahara 4-20-1, Takatsuki, Osaka 569-1094, Japan.

Email: hayashi@gly.oups.ac.jp

Abstract

Objectives: Protease-Activated Receptor (PAR)-1 is a member of a family of G-protein and is activated by a tethered ligand. FR171113, the first non-peptide antagonist of the PAR-1, is effective in preventing occlusive arterial thrombosis without prolonging bleeding time or affecting coagulation time. Obstructive Sleep Apnea (OSA) is a serious sleep disorder that causes cardiovascular disease. Patients with OSA have a high prevalence of atrial fibrillation (AF). This study investigated the influence of FR171113 on cardiac remodeling caused by Intermittent Hypoxia (IH).

Methods: Four-week-old male C57BL/6J mice were exposed to IH (repeated cycles of 5% oxygen for 1.5 min followed by 21% oxygen for 5 min) for 28 days with/without FR171113, a PAR-1 antagonist (1 mg/kg/day).

Results: IH caused an increase of cardiomyocyte cross-sectional area, %fibrosis, 4-HNE-modified protein adducts and superoxide production in the left ventricular myocardium. IH also increased the expression of PAR-1 as well as the phosphorylation of Extracellular Signal-Regulated Kinase (ERK)-1/2 and nuclear factor-kappa B (NF-kB) in human cardiac microvascular endothelial cells. However, FR171113 concentration-dependently suppressed these changes.

Conclusion: FR171113 is able to prevent oxidative stress caused by the IH conditions and ultimately reduces cardiac remodeling by suppressing the activation of ERK-1/2 and NF-kB pathways via PAR-1. Treatment with FR171113 could potentially become an effective therapeutic strategy for cardiac remodeling in patients with OSA and AF.

Introduction

Protease-Activated Receptor (PAR)-1 is a member of a family of G-protein and is activated by a tethered ligand. FR171113, the first non-peptide antagonist of PAR-1, is effective in preventing occlusive arterial thrombosis without prolonging bleeding time or affecting coagulation time [1]. Obstructive Sleep Apnea (OSA) is a serious sleep disorder that leads to Intermittent Hypoxia (IH) and is known to cause cardiovascular disease [2-3]. The hallmark of OSA is the increased production of Reactive Oxygen Species (ROS) in response to IH [4]. ROS can cause interstitial fibrosis and cardiomyocyte hypertrophy [5]. In the previous study, we showed that gp91[phox]-containing NADPH oxidase plays a crucial role in the pathophysiology of IH-induced Left Ventricular (LV) remodeling through an increase of oxidative stress [6]. Patients with OSA have a high incidence of Atrial Fibrillation (AF). On the other hand, OSA has been found to be strikingly more prevalent in patients with AF than in high-risk patients with multiple other cardiovascular diseases [7,8]. Because of this, drugs that prevent thrombosis, such as FR171113, have the potential of showing a positive effect in patients who are suffering from both OSA and AF. However, few studies have reported the effects of FR171113 on the heart under IH conditions.

In our previous study, we showed that FSLLRY, a PAR-2 antagonist, reduced oxidative stress and fibrosis while suppressing the activation of ERK-1/2 and NF-kB pathways via PAR-2 under IH conditions [9]. Although it has been reported that PAR-1 and PAR-2 physically and functionally link to overlapping and distinct profiles of G proteins to differentially regulate downstream signaling pathways [10], substantially little is known about whether PAR-1 antagonist and PAR-2 antagonist can suppress the same signaling pathways on the heart under IH conditions. For the above reasons, we investigated whether FR171113 is able to prevent oxidative stress caused by the IH conditions and ultimately reduce cardiac remodeling. In addition, we also examined whether FR171113 suppresses the activation of ERK-1/2 and NF-kB pathways via PAR-1, similarly to PAR-2 antagonist.

Materials and methods

Experimental protocol

Eight-week-old male C57BL/6J mice (n= 24) were purchased from Japan SLC Inc., (Hamamatsu, Japan). The mice were housed with a 12-h light/dark cycle and with free access to tap water and standard chow. Two intermittent hypoxia groups, a Hypoxia (Hx) group and an Hx-FR171113 group, were created. The mice in the two groups were exposed to IH (5% oxygen for 1.5 min followed by 21% oxygen for 5 min) for 8 h per day during the daytime for 28 consecutive days in a chamber. The normoxia group was exposed to the same ambient noise and lighting conditions as the hypoxia groups. The Hx-FR171113 group was treated with FR171113 (1 mg/kg/day i.p.). After the 28-day experimental period, the heart was excised; the left ventricle was used for light microscopy, immunohistochemistry, and the Reverse Transcription Polymerase Chain Reaction (RT-PCR). The experimental protocol and the handling procedures of the animals were approved beforehand by the Experimental Animal Research Committee of Osaka University of Pharmaceutical Sciences.

Cell culture

Human Cardiac Microvascular Endothelial Cells (HCMECs, LONZA Japan, Tokyo, Japan) were maintained in EGM™-2MV BulletKit™ (LONZA Japan) in 25-cm^2 tissue culture flasks (Becton-Dickinson Ind., NJ, USA) at 37°C under 5% CO_2. These cells were subcultured every 7 days after treatment with 0.25% trypsin/1 mM Ethylenediaminetetraacetic Acid (EDTA) in Ca^{2+}- and Mg^{2+}-free phosphate-buffered saline (PBS). Cells were detached by trypsin digestion, washed once by centrifugation, and resuspended at $5×10^5$ cells/mL in 5 mL of medium per culture flask. Observations were made on the cultures under an inverted light microscope to monitor cell growth and contamination. FR171113 (0.1 μM, 1 μM, 10 μM), or dimethyl sulfoxide was added and incubated for 24 h at 37°C with 5% CO_2 and 20% O_2 or 5% CO_2 and 1% O_2.

Echocardiography

Transthoracic echocardiography was performed using a Vivid E9 instrument (GE Healthcare, Salt Lake City, UT). The LV end-diastolic Diameter (Dd) and the LV end-systolic diameter (Ds), Interventricular Septum Thickness (IVST), and Posterior LV Wall Thickness (PWT) were obtained based on M-mode measurements. The LV mass was calculated using the following formula: LV mass= $0.8×\{1.04×[(Dd+IVST+PWT)^3 - (Dd)^3]\}+0.6$ [11]. The LV Ejection Fraction (EF) was calculated using a modified Simpson's method. In addition, early LV filling velocity (E) of mitral inflow was recorded in the apical four-chamber view with the sample volume near the tips of the mitral leaflets at the site where velocity was maximal and flow was laminar. The early velocity (e') of the mitral annulus was determined by tissue Doppler imaging and the ratio of E to e' (E/e' ratio) was calculated.

Histological examination

For light microscopy, cardiac tissues were fixed in 10% formaldehyde, embedded in paraffin, and cut into 4-μm sections. An ECLIPSE 80i light microscope (Nikon, Tokyo, Japan) was used to take photomicrographs. The cardiac cross-sectional area was evaluated at a magnification of 400× by a previously reported method [12] using ImageJ version 1.44 software (National Institutes of Health, MD, USA). In brief, cardiomyocytes with both a clear nucleus and an intact cell membrane were measured in hematoxylin/eosin-stained nucleated transverse sections, and at least 30 cardiomyocytes were analyzed per heart. After staining with Sirius red, 5 color images were chosen randomly from the high-power fields (200× magnification) and the collagen volume ratio (%) was calculated as described elsewhere [13].

Immunohistochemistry for 4-hydroxy-2-nonenal

Paraffin sections of the left ventricle were subjected to immunohistochemical staining to detect 4-Hydroxy-2-Nonenal (4-HNE) modified protein adducts. Sections were incubated with a monoclonal antibody for 4-HNE (Japan Institute for the Control of Aging, Shizuoka, Japan) and with a secondary antibody (biotinylated anti-mouse IgG), followed by incubation with Vectastain Elite ABC reagent (Vector, CA, USA). The mean area positive for 4-HNE staining was compared with that in the control sections (defined as 1.0).

Detection of superoxide

Freshly frozen unfixed LV myocardial specimens were incubated with 10 μmol/L of dihydroethidium (DHE; Molecular Probes, Eugene, OR, USA) for 30 min at 37°C in a light-protected humidified chamber. After incubation, sections were examined under a BZ-8000 fluorescence microscope (KEYENCE, Osaka, Japan). Detection of *in situ* superoxide production was done by first quantifying DHE fluorescence intensity using NIH Image 1.61 software and then by comparing it with the mean control intensity.

Quantitative real-time RT-PCR

Total RNA was extracted from LV myocardial tissues using TRIzol reagent (Molecular Research Center, OH, USA). Complementary DNA was synthesized from total RNA by reverse transcription using ReverTra Ace qPCR RT Master Mix with cDNA Remover (TOYOBO Co., Ltd., Osaka, Japan). Primers and probes were designed for PAR-1, NF-kB, ERK-1, ERK-2, and GAPDH using ProbeFinder v. 2.45 software (http://qpcr.probefinder.com/roche3.html), a software that is able to create sets of specific primers as well as select TaqMan-locked nucleic acid probes from the Roche Universal Probe Library. The following Universal Probes were purchased from Roche Diagnostics (Basel, Switzerland): No. 69 for mouse PAR-1, No. 76 for human PAR-1, No. 77 for mouse NF-κB, No. 38 for human NF-κB, No. 46 for mouse ERK-1, No.79 for human ERK-1, No. 50 for mouse ERK-2, No.50 for human ERK-2, No. 80 for mouse GAPDH, and No. 80 for human GAPDH. The expression levels of the mRNA were measured using the LightCycler® (Roche Diagnostics). GAPDH was used as the internal standard.

Western blotting

Protein samples (20 μg) were subjected to 12.5% sodium dodecyl sulfate-polyacrylamide gel electrophoresis, followed by electrotransfer of the resolved proteins to a polyvinylidene difluoride membrane (0.45 μm, Merck KGaA, Darmstadt, Germany). The following primary antibodies were used in 1: 1000 dilution: rabbit anti-PAR-1 antibody (Bioss Antibodies Inc., MA, USA), Rabbit anti-PAR-1 antibody (Bioss Antibodies Inc.) Rabbit anti-p-NF-kB primary antibody (Cell Signaling Technology, MA, USA), rabbit anti-NF-kB primary antibody (Santa Cruz Biotechnology, TX, USA), rabbit anti-p-ERK-1/2 primary antibody (Cell Signaling Technology), rabbit anti-ERK-1/2 primary antibody (Cell Signaling Technology), and α-tubulin antibody (Santa Cruz Biotechnology). Reaction products were detected with goat anti-rabbit IgG-peroxidase (4050-05, Southern Biotech, AL, USA) in 1:1000 dilution, and bound peroxidase was visualized using Luminata™ Classico Western horseradish peroxidase (Merck KGaA). Western blotting was performed three times for each sample.

Statistical analysis

Results were expressed as the mean ± Standard Deviation (SD) of the mean. The Tukey-Kramer multiple comparison test was used for statistical analysis and P<0.05 was considered to indicate a significant difference.

Results

Echocardiographic findings

In the Hx group, exposure to IH caused LV diastolic dysfunction. This dysfunction was significantly suppressed in the group treated with FR171113. As a result, there were no significant differences found in the echocardiographic parameters between the Hx-FR171113 group and the normoxia group (Table 1).

Histological findings

In the Hx group, IH caused biventricular cardiomegaly associated with an increase of cardiomyocyte cross-sectional area, myofiber disarray, and fibrosis (Figure 1). These changes were found to have been suppressed in the group that was administered FR171113 (Figures 1-2).

4-HNE and superoxide

In the Hx group, a significant increase of 4-HNE-modified protein adducts and superoxide production (detected by DHE labeling) were seen in the LV myocardium. Both of these changes were significantly suppressed in the group that was administered FR171113 (Figure 1-2).

Real-time RT-PCR findings

In the Hx group, PAR-1, NF-kB, ERK-1 and ERK-2 mRNA levels in the LV were significantly higher than those in the normoxia group. In the Hx-FR171113 group, PAR-1, NF-κB, ERK-1 and ERK-2 mRNA levels were significantly lower than those in the Hx group. No significant differences in the mRNA levels between the normoxia group and the Hx-FR171113 group were observed (Figure 3).

In HCMECs, the PAR-1, NF-kB, ERK-1 and ERK-2 levels in the Hx group were significantly higher than those in the normoxia group. However, the PAR-1, NF-kB, ERK-1 and ERK-2 levels in the Hx-FR171113 group were significantly lower than those in the Hx group. No significant differences in the mRNA expression between the normoxia group and the Hx-FR171113 group were observed (Figure 4).

Western blotting

In HCMECs, the ratios of PAR-1 to α-tubulin, phosphorylated NF-kB (p-NF-kB) to NF-kB, and phosphorylated ERK-1/2 (p-ERK-1/2) to ERK-1/2 in the Hx group were significantly higher than those in the normoxia group. However, these changes were suppressed in a concentration-dependent manner when treated with FR171113. The ratios of PAR-1 to α-tubulin, phosphorylated NF-kB (p-NF-kB) to NF-kB, and phosphorylated ERK-1/2 (p-ERK-1/2) to ERK-1/2 were all significantly suppressed by 10 μM of FR171113 (Figure 5).
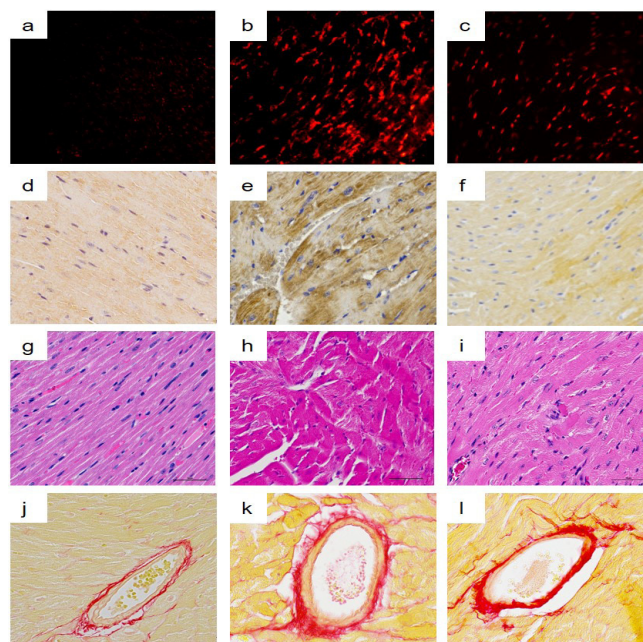

Figure 1: Light micrographs of superoxide production, 4-HNE-modified protein adducts, cardiomyocyte cross-sectional area, and perivascular fibrosis.

Intermittent hypoxia (IH) increased superoxide production (b) and 4-HNE-modified protein adducts (e) in the LV myocardium compared with the normoxia group (a, d). These changes were suppressed by FR171113 (c, f). IH also increased myofiber disarray (h) and perivascular fibrosis (k) in the LV myocardium compared with the normoxia group (g, j). These changes were significantly suppressed by FR171113 (i, l).
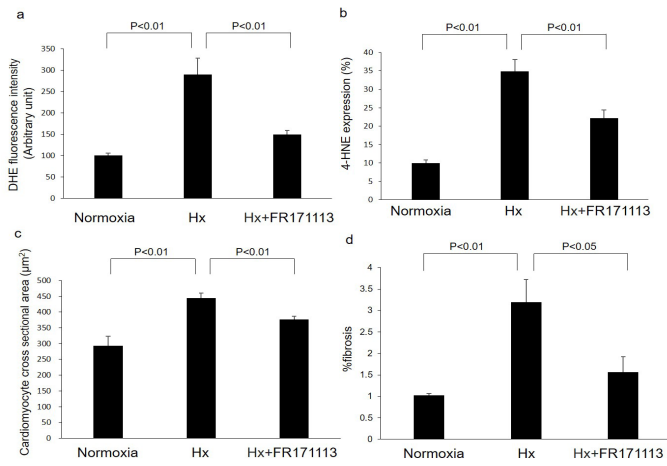
Figure 2: The quantitative measurement of superoxide production, 4-HNE-modified protein adducts, cardiomyocyte cross-sectional area, and perivascular fibrosis.
Intermittent Hypoxia (IH) increased superoxide production (a, n= 4) and 4-HNE-modified protein adducts (b, n= 4) in the LV myocardium compared with the normoxia group. These changes were suppressed by FR171113. IH also significantly increased the cardiomyocyte cross-sectional area (c, n= 4) and perivascular fibrosis (d, n= 4), whereas FR171113 significantly suppressed these changes. Data are shown as the mean and Standard Deviation (SD).
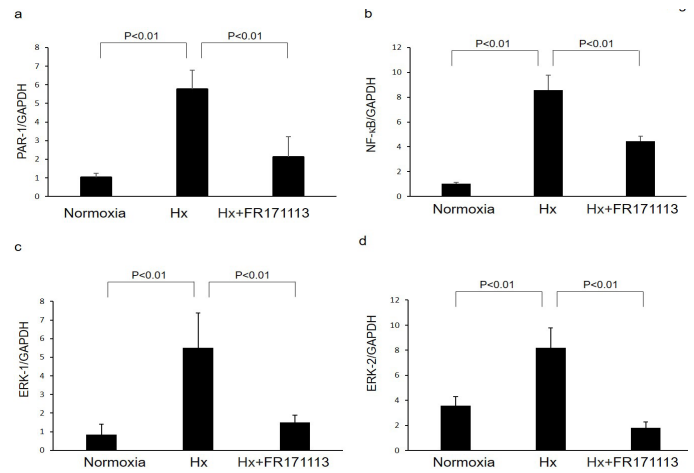
Figure 4: Expression of PAR-1, NF-kB, ERK-1, and ERK-2 in human cardiac microvascular endothelial cells.
Expression of PAR-1 (a, n= 3), NF-kB (b, n= 3), ERK-1 (c, n= 3), and ERK-2 (d, n= 3) mRNAs in human cardiac microvascular endothelial cells was increased by intermittent hypoxia (IH). These changes were significantly suppressed by FR171113. Data are shown as the mean and Standard Deviation (SD).
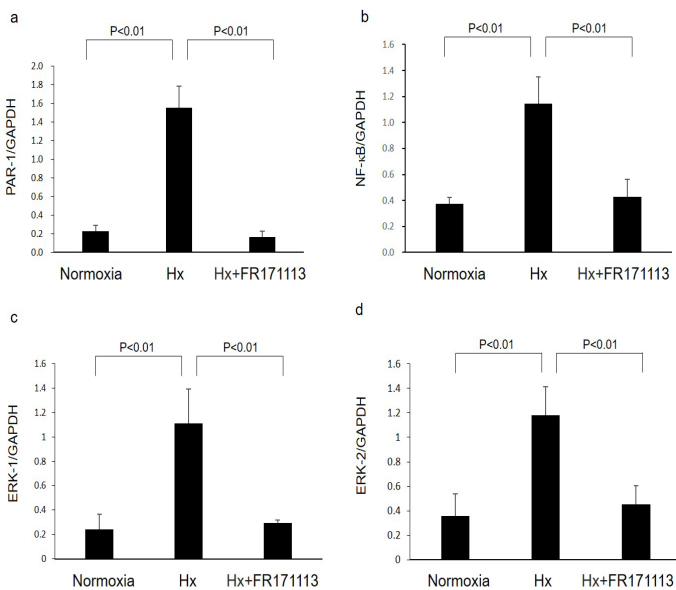
Figure 3: Expression of PAR-1, NF-kB, ERK-1, and ERK-2 mRNAs in the left ventricular myocardial tissues.
Expression of PAR-1 (a, n= 4), NF-kB (b, n=4), ERK-1 (c, n= 4), and ERK-2 (d, n= 4) mRNAs in the left ventricular myocardial tissues was increased by intermittent hypoxia. These changes were significantly suppressed by FR171113. Data are shown as the mean and Standard Deviation (SD).
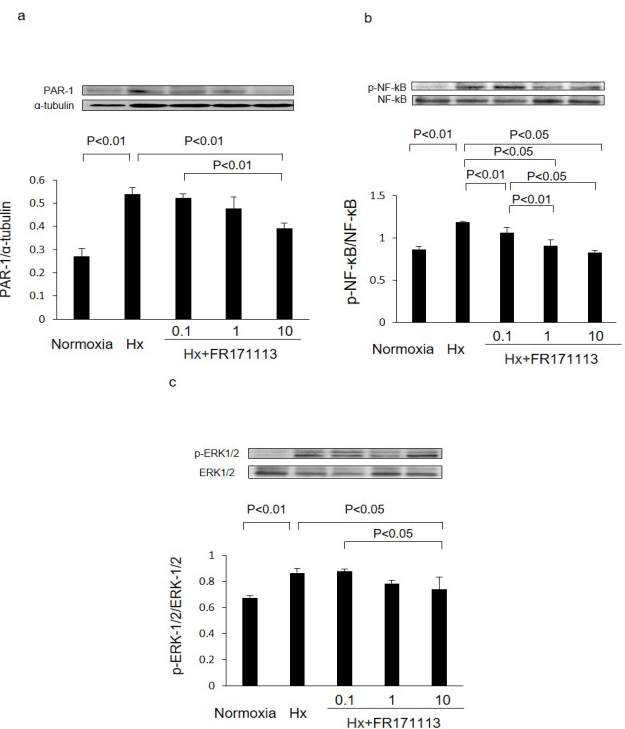
Figure 5: Expression of PAR-1, NF-kB, and ERK-1/2 proteins in human cardiac microvascular endothelial cells.
The ratios of PAR-1 to α-tubulin (a, n= 3), phosphorylated NF-kB (p-NF-kB) to NF-kB (b, n= 3), and phosphorylated ERK-1/2 (p-ERK-1/2) to ERK-1/2 (c, n= 3) in human cardiac microvascular endothelial cells were increased by intermittent hypoxia.These changes were concentration-dependently suppressed by FR171113, when three different concentrations (0.1 μM, 1 μM, and 10 μM) of FR171113 were used in the Hx-FR17113 group. The ratios of PAR-1 to α-tubulin, phosphorylated NF-kB (p-NF-kB) to NF-kB, and phosphorylated ERK-1/2 (p-ERK-1/2) to ERK-1/2 in the Hx-FR17113 group (10 μM) were all significantly lower than those in the Hx group. Data are shown as the mean and Standard Deviation (SD).

Table 1: Echocardiography findings.

	Dd (mm)	Ds (mm)	IVST (mm)	PWT (mm)	LVM (mg)	e' (cm/s)	E/e'	EF (%)
Normoxia	3.75 ± 0.16	2.78 ± 0.11	0.44 ± 0.01	0.44 ± 0.02	39.1 ± 2.1	2.65 ± 0.27	24.9 ± 0.38	56.9±0.7
Hx	3.84 ± 0.26	2.86 ± 0.19	0.45 ± 0.03	0.45 ± 0.00	42.2 ± 4.7	2.03 ± 0.32	30.7 ± 3.02[*]	53.7±2.8
Hx + FR171113	3.75 ± 0.11	2.88 ± 0.08	0.43 ± 0.02	0.44 ± 0.02	38.5 ± 1.3	2.26 ± 0.02	26.1 ± 1.17[ŧ]	52.0±1.2

Dd, Left Ventricular (LV) end-diastolic diameter; Ds, LV end-systolic diameter; IVST, interventricular septum thickness; PWT, posterior LV wall thickness; LVM, LV mass; E, early rapid filling wave of mitral inflow velocity; e', early velocity of the mitral annulus; EF, LV ejection fraction; Hx, hypoxia. LVM was calculated using the following formula: $LVM = 0.8 \times \{1.04 \times [(Dd+IVST+PWT)^3 - (Dd)^3]\} + 0.6$. Data are shown as the mean ± SD (n= 3-4). [*]$P<0.05$, compared with Normoxia. ŧ$P<0.05$, compared with Hx.

Discussion

This study showed that the exposure of mice to IH conditions leads to cardiomyocyte hypertrophy and perivascular fibrosis in the LV myocardium. It was also shown that treatment with FR171113 reduces the level of these damages. Impairment of LV diastolic function has been multiply reported in patients with OSA [3,14]. The same condition of LV diastolic dysfunction was developed in mice, when exposed to IH conditions for 4 weeks in our study. These changes that were caused by IH conditions were reduced in the mice that received FR171113, suggesting that the suppression of PAR-1 is important in preventing damages that occur in the LV myocardium under IH conditions. Although the change in LV mass was small, it was considered because it depends on time exposed to IH. The research under exposure of IH for longer time will be conducted in our future study.

In our previous study, we showed that NADPH-dependent superoxide production was significantly increased by IH causing the development of cardiac hypertrophy in mice [6] and that scavenging ROS by hydrogen gas inhalation attenuated cardiac remodeling [15,16]. These results suggested that suppressing ROS is important in preventing damages caused by IH in the LV myocardium. In the present study, we showed that the PAR-1 expression is increased by IH and that this change can be suppressed by treatment with FR171113. In addition, the production of ROS induced by IH was also suppressed by FR171113. PAR-1 has been reported to produce ROS amount via NADPH oxidase [17]. As a PAR-1 antagonist, FR171113 is considered to suppress cardiac remodeling by efficiently reducing the production of ROS through the inhibition of PAR-1.

We also showed in this study that FR171113 reduces cardiomyocyte cross-sectional area and fibrosis increased by IH. NADPH oxidase induces cardiac fibrosis and hypertrophy through activating NF-kB signaling pathways [18]. NF-kB activation is mediated through PAR1-mediated MAPKs in human cardiomyocytes [19]. Cardiac hypertrophy is regulated by the ERK pathway [20]. In this study, we also showed that the ratios of PAR-1 to α-tubulin, p-NF-kB to NF-kB, and p-ERK-1/2 to ERK-1/2 increased by IH were concentration-dependently suppressed by FR171113. These findings indicate that FR171113 can prevent cardiac hypertrophy and fibrosis by suppressing the activation of ERK-1/2 and NF-kB pathways via PAR-1 under IH conditions.

We also examined the expression of PAR-1, NF-kB, ERK-1 and ERK-2 mRNAs under IH conditions. The expression of these mRNAs in the Hx-FR171113 group was significantly lower than that in the Hx group. These findings indicate that when ERK-1/2 and NF-kB signaling pathways via PAR-1 are activated in IH conditions, the gene expression levels of the molecules responsible for these pathways are upregulated. In other words, once signaling pathways via PAR-1 are activated under IH conditions, the signaling activation is considered to further enhance. This shows the importance of suppressing the signaling pathways via PAR-1 under IH conditions in order to protect cardiac tissues.

In this study, we showed that FR171113, a PAR-1 antagonist, is able to prevent oxidative stress caused by IH conditions and ultimately reduce cardiac remodeling by suppressing the activation of ERK-1/2 and NF-kB pathways via PAR-1. As mentioned earlier, in our previous study, we also showed that FSLLRY, a PAR-2 antagonist, suppressed the activation of ERK-1/2 and NF-kB pathways via PAR-2 under IH conditions (9). The results of these two studies indicate that both PAR-1 antagonist and PAR-2 antagonist can suppress the same signaling pathways on the heart under IH conditions. Therefore, it is considered that anticoagulant drugs with inhibitory effect on either PAR-1 or PAR-2 (at least one) have the possibility of contributing to prevent cardiac remodeling in patients with OSA and AF. Although a more detailed investigation needs to be conducted for the elucidation of the cardioprotective effects of PAR-1 and PAR-2 antagonists, therapies targeting PAR-1 and PAR-2 are considered to have the potential to be useful for huge patients exposed to hypoxia or ischemia.

Conclusion

FR171113, a PAR-1 antagonist, was able to reduce oxidative stress in the myocardium, consequently attenuating cardiomyocyte hypertrophy caused by IH. Drugs like FR171113 that have an effect of suppressing the expression of PAR-1 gene, have the possibility of suppressing the IH-induced changes by effectively reducing oxidative stress. These findings suggest that FR171113 could be a potentially effective treatment for the prevention of cardiac remodeling in patients with OSA and AF.

Acknowledgments

References

1. Kato Y, Kita Y, Hirasawa-Taniyama Y, Nishio M, Mihara K, et al. Inhibition of arterial thrombosis by a protease-activated recep-

tor 1 antagonist, FR171113, in the guinea pig. Eur J Pharmacol. 2003; 25: 163-169.

2. Kato M, Adachi T, Koshino Y, Virend K. Obstructive sleep apnea and cardiovascular disease. Circ J. 2009; 73: 1363-1370.

3. Lattimore JDL, David S, Wilcox I. Obstructive sleep apnea and cardiovascular disease. J Am Coll Cardiol. 2003; 41: 1429-1437.

4. Christou K, Markoulis N, Moulas AN, Pastaka C, Gourgoulianis KI. Reactive Oxygen Metabolites (ROMs) as an index of oxidative stress in obstructive sleep apnea patients. Sleep Breath. 2003; 7: 105-110.

5. Siwik DA, Tzortzis JD, Pimental DR, Chang DLF, Pagano PJ, et al. Inhibition of copper-zinc superoxide dismutase induces cell growth, hypertrophic phenotype, and apoptosis in neonatal rat cardiac myocytes in vitro. Circ Res. 1999; 85: 147-153.

6. Hayashi T, Yamashita C, Matsumoto C, Kwak CJ, Fujii K, et al. Role of gp91phox-containing NADPH oxidase in left ventricular remodeling induced by intermittent hypoxic stress. Am J Physiol Heart Circ Physiol. 2008; 294: 2197-2203.

7. Szymanski FM, Płatek AE, Karpinski G, Kozluk E, Puchalski B, et al. Obstructive sleep apnoea in patients with atrial fibrillation: prevalence, determinants and clinical characteristics of patients in Polish population. Kardiol Pol. 2014; 72: 716-724.

8. Gami AS, Pressman G, Caples SM, Kanagala R, Gard JJ, et al. Association of atrial fibrillation and obstructive sleep apnea. Circulation. 2004; 110: 364-367.

9. Imano H, Kato R, Tanikawa S, Yoshimura F, Nomura A, et al. Factor Xa inhibition by rivaroxaban attenuates cardiac remodeling due to intermittent hypoxia. J Pharmacol Sci. 2018; 137: 274-282.

10. McCoy KL, Traynelis SF, Hepler JR. PAR1 and PAR2 couple to overlapping and distinct sets of G proteins and linked signaling pathways to differentially regulate cell physiology. Mol Pharmacol. 2010; 77: 1005-1015.

11. Devereux RB, Alonso DR, Lutas EM, Gottlieb GJ, Campo E, et al. Echocardiographic assessment of left ventricular hypertrophy: comparison to necropsy findings. Am J Cardiol. 1986; 57: 450-458.

12. Duran JM, Makarewich CA, Trappanese D, Gross P, Husain S, et al. Sorafenib cardiotoxicity increases mortality after myocardial infarction. Circ Res. 2014; 114: 1700-1712.

13. Yamashita C, Hayashi T, Mori T, Tazawa N, Kwak CJ, et al. Angiotensin-II receptor blocker reduces oxidative stress and attenuates hypoxia-induced left ventricular remodeling in apolipoprotein E-knockout mice. Hypertens Res. 2007; 30: 1219-1230.

14. Kasai T. Sleep apnea and heart failure. J Cardiol. 2012; 60: 78-85.

15. Inamoto S, Yoshioka T, Yamashita C, Miyamura M, Mori T, et al. Pitavastatin reduces oxidative stress and attenuates intermittent hypoxia-induced left ventricular remodeling in lean mice. Hypertens Res. 2010; 33: 579-586.

16. Hayashi T, Yoshioka T, Hasegawa K, Miyamura M, Mori T, et al. Inhalation of hydrogen gas attenuates left ventricular remodeling induced by intermittent hypoxia in mice. Am J Physiol Heart Circ Physiol. 2011; 301: H1062-H1069.

17. Huang QT, Chen JH, Hang LL, Liu SS, Zhong M. Activation of PAR-1/NADPH oxidase/ROS signaling pathways is crucial for the thrombin-induced sFlt-1 production in extravillous trophoblasts: possible involvement in the pathogenesis of preeclampsia. Cell Physiol Biochem. 2015; 35: 1654-1662.

18. Zhao QD, Viswanadhapalli S, Williams P, Shi Q, Tan C, et al. NADPH oxidase 4 induces cardiac fibrosis and hypertrophy through activating Akt/mTOR and NFkB signaling pathways. Circulation. 2015; 131: 643-655.

19. Chien PT, Hsieh HL, Chi PL, Yang CM. PAR1-dependent COX-2/PGE2 production contributes to cell proliferation via EP2 receptors in primary human cardiomyocytes. Br J Pharmacol. 2014; 171: 4504-4519.

20. Hu B, Song JT, Ji XF, Liu ZQ, Cong ML, et al. Sodium Ferulate Protects against Angiotensin II-Induced Cardiac Hypertrophy in Mice by Regulating the MAPK/ERK and JNK Pathways. Biomed Res Int. 2017; 2017: 3754942.